



Tom Milligan
Milligan & Associates
8204 West Polk Place
Littleton, CO 80123
(303) 977-7268
(303) 977-8853 (Fax)
TMilligan@ieee.org (e-mail)

Design of Corrugated Horns: A Primer

Christophe Granet and Graeme L. James

CSIRO ICT Centre, Electromagnetics & Antennas
PO Box 76, Epping 1710, NSW, Australia
E-mail: Christophe.Granet@csiro.au

Keywords: Corrugated horn antennas; antenna feeds; reflector antenna feeds

1. Introduction

Over the past 40 years, corrugated horns supporting so-called hybrid modes have become well established as feeds for reflector antennas, and even as direct radiators. It is not difficult to trace the popularity of the corrugated horn, given the ability of certain hybrid modes to produce radiation patterns having extremely good beam symmetry with low cross-polarization levels, a high beam efficiency with very low sidelobes, and the potential for wide-bandwidth performance [1, 2]. Why they are called "corrugated" is clear from the typical example of a horn shown in Figure 1, where the inside wall is manufactured in a succession of slots and "teeth." The purpose of the corrugated surface is to provide the means to support the propagation of hybrid modes within the horn. Hybrid modes are basically a combination of TE and TM

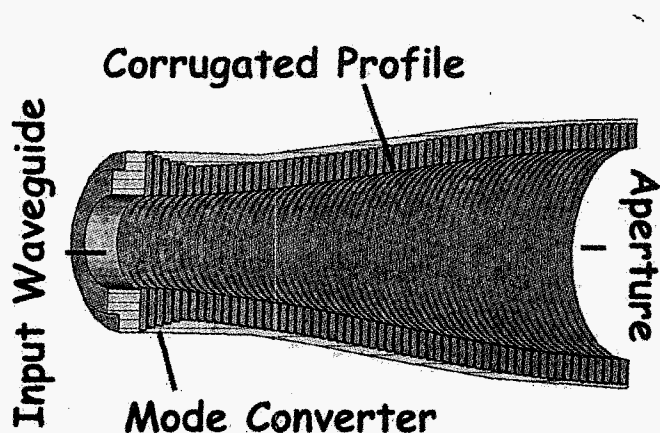


Figure 1a. A cut-away view of a typical corrugated horn.

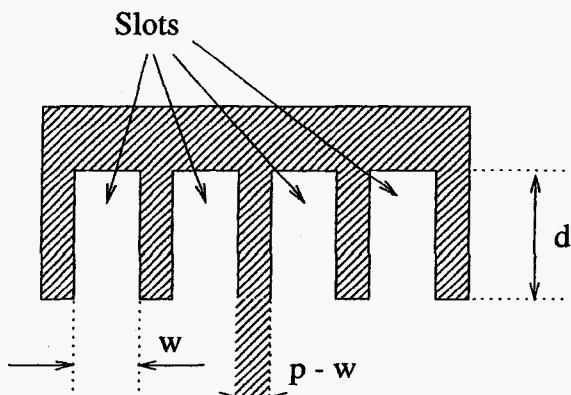


Figure 1b. The details of the corrugated inside wall of a typical corrugated horn.

modes. For this combination to propagate as a single entity with a common propagating velocity, the horn or waveguide must have anisotropic surface-reactance properties: properties that are satisfied by the corrugated surface. It is worth pointing out that hybrid modes can also be supported by other means, such as waveguides or horns partially filled with dielectric [1]. However, these alternative possibilities are outside the scope of this design note.

There have been many papers relating to the theoretical description of corrugated horns, but relatively few giving tips on how to easily come up with a good, basic design that can then be optimized, either by trial and error or directly through an automated optimization algorithm. In an attempt to fill this gap, we provide here some basic information for the inexperienced horn designer to get started in designing their first corrugated horn. The starting procedure outlined here is based on our combined experience in designing high-efficiency corrugated horns for numerous

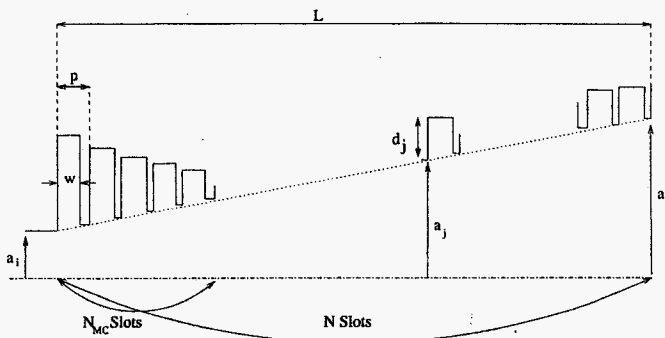


Figure 2a. The geometrical parameters of a corrugated horn with a variable-depth mode converter.

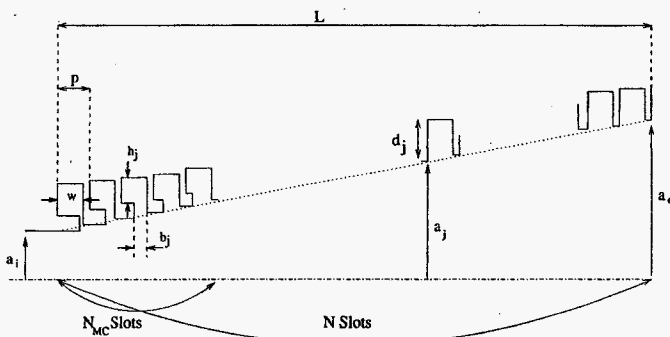


Figure 2b. The geometrical parameters of a corrugated horn with a ring-loaded slot mode converter.

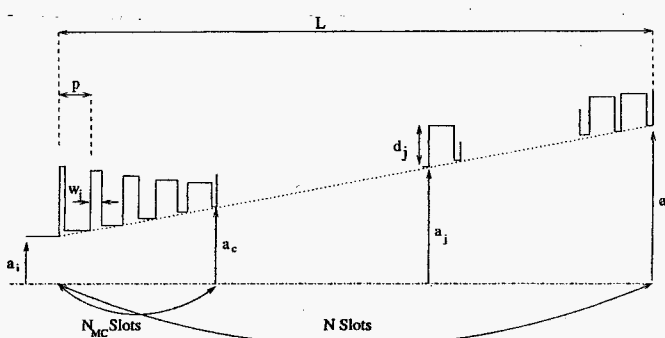


Figure 2c. The geometrical parameters of a corrugated horn with a variable-pitch-to-width mode converter.

Table 1. Corrugated-horn parameters.

Quantity	Symbol
Input radius	a_i
Output radius	a_o
Length	L
Total number of slots	N
Number of slots in the mode converter	N_{MC}
Slot pitch	$p = L/N$
Slot width	w
Slot pitch-to-width ratio	$\delta = w/p$
Width of the slot teeth	$(p - w) = (1 - \delta)p$
Depth of the j -th slot	d_j where $1 \leq j \leq N$

applications over many years. Other experienced horn designers have, undoubtedly, different design starting points, but the following tips have always worked well for us.

We begin with some practical considerations. The bandwidth of a horn is usually defined by the frequency range over which the horn is required to have a suitable beamwidth and beam symmetry for a return loss usually better than 15 to 18 dB, and with a cross-polarization maximum better than -20 to -25 dB. These values are typical, but many high-performance applications have much tighter specifications. Remember that the following procedure is only designed to provide a good starting point.

For a standard application, the hybrid mode normally required in the horn is the HE_{11} mode where, in a well-designed feed or direct radiator, the resulting radiation pattern is very close to a Gaussian-shaped pattern. It is this Gaussian-pattern characteristic that we wish to maintain over the operating bandwidth of the horn, in order to satisfy the cross-polarization, return-loss, and sidelobe requirements for the given application.

As illustrated in Figure 1, it is usual for the corrugated horn to be connected to a circular, smooth-walled, input waveguide. The fundamental mode of this guide is the TE_{11} mode, and there is the need for a so-called "mode converter" at the transition between the smooth-walled input waveguide and the body of the corrugated horn. This mode converter is designed to provide a smooth transition from the TE_{11} to the HE_{11} mode supported by the corrugated horn.

To conclude our initial comments, the corrugated horns considered here have their slots perpendicular to the axis of the horn, as shown in Figure 1, and are to be used mainly as feeds for Cassegrain or Gregorian reflector antennas, or as direct radiators. For this reason, it is assumed that the aperture diameter is to be around two wavelengths or more in dimension.

2. Design Parameters

We consider the class of circularly symmetrical corrugated horns illustrated in Figures 1 and 2. There are quite a number of quantities to define in the design of corrugated horns [3-7], with the main ones listed in Table 1. Aside from these quantities, there are several other parameters to consider. First, we have the following four frequencies to aid in the design:

- f_{min} : lowest operating frequency
- f_{max} : highest operating frequency (where $f_{max} \leq 2.4f_{min}$)
- f_c : the “center frequency” (wavelength λ_c)
- f_o : the “output frequency” (wavelength λ_o)

The other main parameters to consider are:

- Choice of the input radius
- Choice of the output radius
- Choice of the depths of the slots
- Choice of corrugation pitch and pitch-to-width ratio
- Choice of the mode converter
- Choice of horn length
- Choice of the corrugated-surface profile
- Phase-center position.

We will now consider each of these parameters in turn.

2.1 Center Frequency and Output Frequency

The choice of these frequencies depends on whether the horn is for narrowband or broadband applications.

2.1.1 Narrow-Band Applications Where $f_{max} \leq 1.4f_{min}$

The center frequency, f_c , is usually chosen to be $f_c = \sqrt{f_{min}f_{max}}$. The output frequency, f_o , (i.e., the last slot of the horn is optimized for a nominal $\frac{\lambda_o}{4}$) is usually chosen to be $f_c \leq f_o \leq 1.05f_c$.

2.1.2 Broadband Applications Where $1.4f_{min} \leq f_{max} \leq 2.4f_{min}$

In this case, these frequencies are chosen to be $f_c \approx 1.2f_{min}$ and $1.05f_c \leq f_o \leq 1.15f_c$.

2.2 Input Radius

The fundamental mode in a circular waveguide is the TE₁₁ mode, which has a cut-off wavenumber

$$k = \frac{2\pi}{\lambda} = \frac{1.841}{\text{radius of circular waveguide}}.$$

Therefore, the input radius, a_i , of a corrugated horn must satisfy the inequality $\frac{2\pi f_{min}}{c} a_i \geq 1.84118$ (where c is the speed of light), and is often chosen to be such that

$$k_c a_i = \frac{2\pi}{\lambda_c} a_i = 3, \text{ i.e., } a_i = \frac{3\lambda_c}{2\pi}.$$

This choice of a_i usually insures a return loss of the horn of over 15 dB at f_{min} .

2.3 Output Radius

Typically, a corrugated horn is designed to have a taper of between -12 dB to -18 dB at an angle corresponding to the edge of the reflector or the edge of the target being illuminated. Figure 3 gives an estimate of the output radius, a_o , (in λ_c) at edge-taper values of -12, -15, and -18 dB for half-subtended angles between 15° and 40°.

2.4 Nominal Slot-Depth Calculation

The design of corrugations in a corrugated horn is very important for providing good performance. One of the most important parameters is the depth of the slot along the length of the horn.

The corrugated surface of a corrugated horn represents a surface reactance, χ_j , at a point along the horn where the radius is a_j and the slot-depth is d_j , defined by [3]

$$\chi_j = -\delta \frac{J_1(k_c a_j) Y_1[k_c(a_j + d_j)] - Y_1(k_c a_j) J_1[k_c(a_j + d_j)]}{J'_1(k_c a_j) Y_1[k_c(a_j + d_j)] - Y'_1(k_c a_j) J_1[k_c(a_j + d_j)]}, \quad (1)$$

where $k_c = \frac{2\pi}{\lambda_c}$, J_1 is the Bessel function of the first kind of order one (J'_1 is its derivative), and Y_1 is the Bessel function of the second kind of order one (Y'_1 is its derivative).

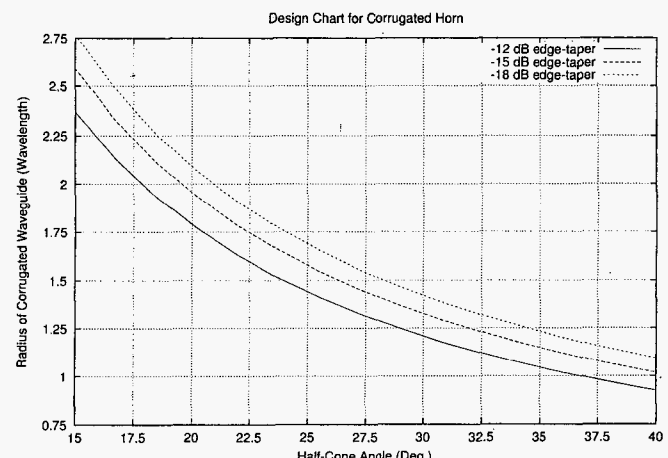


Figure 3. An estimate of the output radius for a given taper at a given illumination angle.

When $\|\chi_j\| \rightarrow \infty$, then the HE_{1n} or EH_{1n} modes are said to be in the balanced hybrid condition. To arrive at that condition, the denominator of Equation (1) will have to be zero or infinitesimally small. It is therefore useful to solve

$$J'_1(k_c a_j) Y_1[k_c(a_j + d_j)] - Y'_1(k_c a_j) J_1[k_c(a_j + d_j)] = 0. \quad (2)$$

A plot of the solutions $(k_c d_j)$ of this equation is shown in Figure 4 for values of $(k_c a_j)$ between two and 40. The solution of this equation is often said to be that d_j should be nominally equal to $\lambda_c/4$, but a better solution can be obtained. Using the solutions of $(k_c d_j)$ of Equation (2), a correction factor, κ [7], is applied to $\lambda_c/4$, i.e., the solution of Equation (2) for a given $(k_c a_j)$ is

$$d_j = \kappa \frac{\lambda_c}{4}. \quad (3)$$

We can approximate the value of κ by the expression

$$\kappa = \exp \left[\frac{1}{2.114(k_c a_j)^{1.134}} \right]. \quad (4)$$

A comparison of Equation (4) and the theoretical value of κ is shown in Figure 5, where it can be seen that the use of Equation (4) gives an excellent approximation of the required correction factor.

In a more sophisticated application of the corrugated horn, we can utilize the slot depth for multi-band purposes. The surface-reactance conditions necessary to support the dominant hybrid mode occur at frequencies in the vicinity of wavelengths where the slot depth is $n\lambda/4$, where n is an odd integer. Thus, the first multi-band pair occurs at frequencies where the slot depth is around $\lambda/4$ in the lower band and at around $3\lambda/4$ in the upper band. One multi-band application of such "deep slots" is given in [8], where the slot depth, d_j , corresponds to a nominal $3\lambda/4$ at the lowest frequency band and a nominal $5\lambda/4$ at the highest frequency band. Assuming that the principal frequency range is the lowest part of

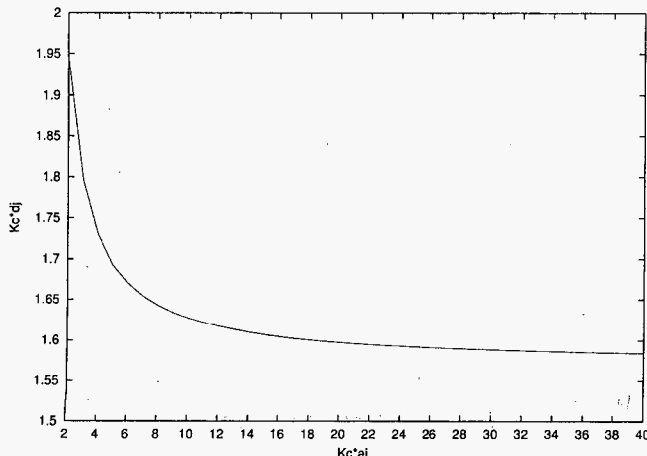


Figure 4. The solutions $(k_c d_j)$ of Equation (2) for $\|\chi_j\| \rightarrow \infty$.

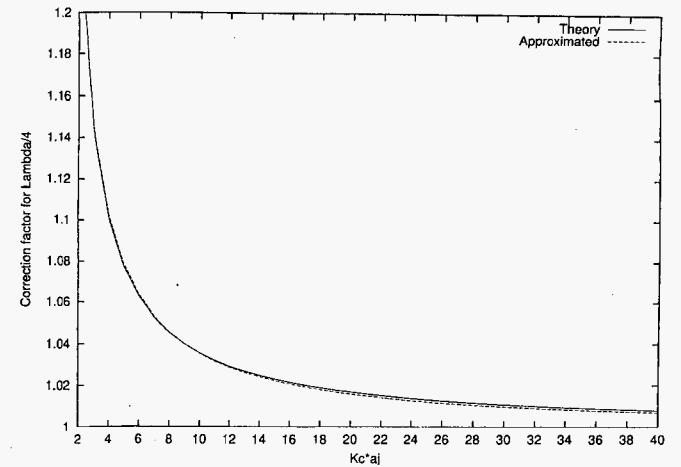


Figure 5. The approximated expression for κ compared to the theoretical value for a nominal slot depth of $\frac{\lambda_c}{4}$.

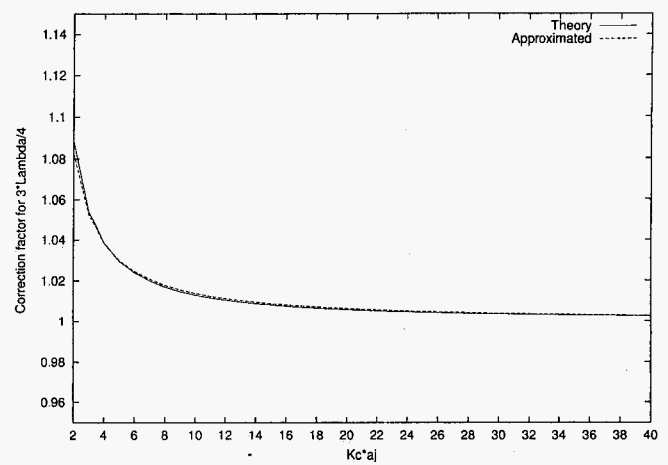


Figure 6. The approximated expression for κ compared to the theoretical value for a nominal slot depth of $\frac{3\lambda_c}{4}$.

the band, the correction factor, κ , for this kind of slot depth ($d_j = \kappa \frac{3\lambda}{4}$) is given by

$$\kappa = \exp \left[\frac{1}{5.955(k_c a_j)^{1.079}} \right]. \quad (5)$$

A comparison of Equation (5) and the theoretical value of κ is shown in Figure 6, where it can be seen that the use of Equation (5) gives (as in the previous example) an excellent approximation of the required correction factor.

A note of caution in using deep slots: as the value of n increases, the bandwidth capabilities of the upper band(s) become increasingly restricted. In addition, the performance of the horn in these upper bands is usually somewhat poorer than for the lower band, and additional optimization is often necessary to achieve a usable result.

Table 2a. The slot-depth calculations for a variable-depth-slot mode converter (Figure 2a).

When $1 \leq j \leq N_{MC} + 1$, then the slot depth of the j th slot is

$$d_j = \left\{ \sigma - \frac{j-1}{N_{MC}} \left(\sigma - \frac{1}{4} \exp \left[\frac{1}{2.114(k_c a_j)^{1.134}} \right] \right) \right\} \lambda_c$$

where σ ($0.4 \leq \sigma \leq 0.5$) is a percentage factor for the first slot depth of the mode converter.

When $N_{MC} + 2 \leq j \leq N$, then the slot depth of the j th slot is

$$\begin{aligned} d_j = & \frac{\lambda_c}{4} \exp \left[\frac{1}{2.114(k_c a_j)^{1.134}} \right] \\ & - \left(\frac{j-N_{MC}-1}{N-N_{MC}-1} \right) \left\{ \frac{\lambda_c}{4} \exp \left[\frac{1}{2.114(k_c a_o)^{1.134}} \right] \right. \\ & \left. - \frac{\lambda_o}{4} \exp \left[\frac{1}{2.114(k_o a_o)^{1.134}} \right] \right\} \end{aligned}$$

Table 2b. The slot-depth calculations for a ring-loaded-slot mode converter (Figure 2b). [As the details of a ring-loaded-slot mode converter are more complex, we have shown, for illustration purposes, the geometry of a typical five-ring-loaded-slot mode converter in Figure 7.]

When $1 \leq j \leq N_{MC} + 1$, then the slot depth of the j th slot is

$$d_j = \frac{\lambda_c}{4} \exp \left[\frac{1}{2.114(k_c a_j)^{1.134}} \right].$$

When $N_{MC} + 2 \leq j \leq N$, then the slot depth of j th slot is

$$\begin{aligned} d_j = & \frac{\lambda_c}{4} \exp \left[\frac{1}{2.114(k_c a_j)^{1.134}} \right] \\ & - \left(\frac{j-N_{MC}-1}{N-N_{MC}-1} \right) \left\{ \frac{\lambda_c}{4} \exp \left[\frac{1}{2.114(k_c a_o)^{1.134}} \right] \right. \\ & \left. - \frac{\lambda_o}{4} \exp \left[\frac{1}{2.114(k_o a_o)^{1.134}} \right] \right\}. \end{aligned}$$

When $1 \leq j \leq N_{MC}$, then the width of the b_j th slot is

$$b_j = \left[0.1 + (j-1) \frac{\delta - 0.1}{N_{MC}} \right] p,$$

and the height of the h_j th slot is

$$h_j = \frac{2}{3} d_j.$$

Table 2c. The slot-depth calculations for a variable-pitch-to-width-slot mode converter (Figure 2c).

When $1 \leq j \leq N_{MC} + 1$, then the slot depth of the j th slot is

$$d_j = \left[\sigma \frac{\lambda_c}{1.15} + \frac{j-1}{N_{MC}-1} \left(\frac{\lambda_c}{4} - \sigma \frac{\lambda_c}{4} \right) \right] \exp \left[\frac{1}{2.114(k_c a_j)^{1.134}} \right].$$

When $N_{MC} + 2 \leq j \leq N$, then the slot depth of the j th slot is

$$\begin{aligned} d_j = & \frac{\lambda_c}{4} \exp \left[\frac{1}{2.114(k_c a_j)^{1.134}} \right] \\ & - \left(\frac{j-N_{MC}-1}{N-N_{MC}-1} \right) \left\{ \frac{\lambda_c}{4} \exp \left[\frac{1}{2.114(k_c a_o)^{1.134}} \right] \right. \\ & \left. - \frac{\lambda_o}{4} \exp \left[\frac{1}{2.114(k_o a_o)^{1.134}} \right] \right\}. \end{aligned}$$

When $1 \leq j \leq N_{MC}$, then the width of the w_j th slot is

$$w_j = \delta_{min} + \frac{j-1}{N_{mc}-1} (\delta_{max} - \delta_{min}),$$

with $0.125 \leq \delta_{min} \leq \delta$ and $\delta_{max} \approx \delta$ (the nominal pitch-to-width ratio).

As before, $0.4 \leq \sigma \leq 0.5$.

2.5 Pitch and Pitch-to-Width Ratio

The pitch, p , is usually chosen to be such that $\frac{\lambda_c}{10} \leq p \leq \frac{\lambda_c}{5}$.

For narrowband operation, a pitch closer to $\lambda_c/5$ is acceptable, while for broadband applications, a pitch closer to $\lambda_c/10$ is preferable.

The pitch-to-width ratio, δ , is usually taken to be $0.7 \leq \delta \leq 0.9$. This parameter mostly influences the level of cross-polarization [1, 2].

2.6 Mode Converter

Usually, the input waveguide is excited by a pure TE₁₁ mode (at least that is what the horn designer would like!), and a mode converter is required to do the TE₁₁-to-HE₁₁ mode conversion over a specified number of slots. There are basically three types of mode converters to choose from, as shown in Figure 2. The choice is important, and is made, keeping the required bandwidth in mind, as follows:

- i) variable-depth-slot mode converter [3, 5, 6] for $f_{max} \leq 1.8 f_{min}$ (the most commonly used mode converter);
- ii) ring-loaded-slot mode converter [4, 6] for $f_{max} \leq 2.4 f_{min}$;

- iii) variable-pitch-to-width-slot mode converter [9] for $f_{max} \leq 2.05 f_{min}$ (used occasionally by some horn designers).

In the following, we will assume that nominal quarter-wavelength slot depths are used, and we will apply the corresponding correction factor, κ .

In practice, the number of slots, N_{MC} , in a mode converter is typically $5 \leq N_{MC} \leq 7$ for mode converters i) and ii), and $7 \leq N_{MC} \leq 12$ for the mode converter in iii). The slot-depth calculations for the three types of mode converter are given in Table 2.

2.7 Choice of Horn Length

The length of the horn is usually set by the application, but around $5\lambda_c$ to $10\lambda_c$ is usually required, although some applications may need a horn $20\lambda_c$ to $30\lambda_c$ long. The length will have an impact on the sidelobes and the stability of the phase center of the horn. Some experimentation is usually needed. In some cases, designs are optimized to be as compact as possible to reduce cost and weight, especially for onboard satellite applications.

2.8 Choice of the Corrugated Surface Profile

In Table 3 we summarize a variety of profile options available to the feed-horn designer. These profiles are taken from [10], but are repeated here for completeness. The most commonly used profiles are the first three in the table, with the linear profile being simply that of the conical corrugated horn. The parameter ρ , appearing in some of these profiles, is generally equal to two, but taking values such that $0.5 \leq \rho \leq 5$ gives rise to interesting profiles with their own sets of properties. The idea here is to provide a set of possible profiles and to let the reader experiment to work out which one best fits the application's specifications. Some horn designers also use combinations of such profiles [11]. Lately, the so-called Gaussian profile (equivalent to the hyperbolic profile) has been used extensively [12]. This horn profile usually displays good pattern characteristics.

2.9 Phase-Center Position

The phase-center position within the horn is determined from the variation in phase across the horn aperture. As this can be affected by a number of factors, we can only prescribe a very rough "rule of thumb" for a general estimation of the phase center to cover all possible horn designs considered here. The final position should be determined experimentally, or from further numerical analysis. As a useful starting point, the phase-center position, as measured from the aperture towards the apex of the horn, is given by αL , where $0 \leq \alpha \leq 1$, and is approximated by

$$\alpha = 1 - \exp \left[-4.8 \left(\frac{k_c a_o^2}{4\pi L} \right)^2 \right].$$

As a general rule, narrowband horns tend to have their phase centers near the aperture, and for broadband horns, the phase center moves towards the apex of the horn. In a well-designed broadband horn, the phase center remains relatively static, at a position close to the apex.

3. Analysis Methods

There are several ways of analyzing the performance of a corrugated horn. The most widely used technique is the mode-matching method [3]. However, if you do not have ready access to such a technique, more general programs are now becoming available. These include (to name only a few, apologies for omissions) Ansoft HFSS, CST MicroWave Studio, WASPnet, WIPL-D, and Mician MicroWave Wizard. Using the guidelines in this article, it is possible to generate a basic corrugated-horn geometry easily, and to follow this with a refined parameter study using one of the available software packages in an attempt to obtain the required performance specific to your application.

Table 3. Some types of corrugated surface profiles.

Profile	Formulation
Linear	$a(z) = a_i + (a_o - a_i) \frac{z}{L}$
Sinusoid	$a(z) = a_i + (a_o - a_i) \left[(1 - A) \frac{z}{L} + A \sin^2 \left(\frac{\pi z}{2L} \right) \right]$ where $A \in [0;1]$
Asymmetric sine-squared	$a(z) = a_i + \frac{2(a_o - a_i)}{1 + \gamma} \sin^2 \left(\frac{\pi z}{4L_1} \right)$ for $0 \leq z \leq L_1$; $a(z) = a_i + \frac{2(a_o - a_i)}{1 + \gamma} \left\{ \gamma \sin^2 \left[\frac{\pi(z + L_2 - L_1)}{4L_2} \right] + \frac{1 - \gamma}{2} \right\}$ for $L_1 \leq z \leq L$, $L = L_1 + L_2$, and $\gamma = \frac{L_2}{L_1}$.
Tangential	$a(z) = a_i + (a_o - a_i) \left[(1 - A) \frac{z}{L} + A \tan^2 \left(\frac{\pi z}{4L} \right) \right]$ where $A \in [0;1]$
xp	$a(z) = a_i + (a_o - a_i) \left[(1 - A) \frac{z}{L} + A \left(\frac{z}{L} \right)^\rho \right]$ where $A \in [0;1]$
Exponential	$a(z) = a_i \exp \left[\ln \left(\frac{a_o}{a_i} \right) \frac{z}{L} \right]$
Hyperbolic	$a(z) = \sqrt{a_i^2 + \frac{z^2 (a_o^2 - a_i^2)}{L^2}}$
Polynomial	$a(z) = a_i + (\rho + 1)(a_o - a_i) \left[1 - \frac{\rho z}{(\rho + 1)L} \right] \left(\frac{z}{L} \right)^\rho$

4. Example

As an example, consider a standard Ku-band operation from a typical Earth station. We assume the Earth station is a Cassegrain antenna (made of a parabolic main reflector and an ellipsoidal subreflector), with a requirement to receive satellite signals in the 10.7-12.75 GHz frequency band, and to transmit signals in the 14.0-14.5 GHz band. The half-subtended angle from the focus of the antenna to the subreflector is 20°, and a -15 dB edge taper on the feed pattern is specified at this angle.

So, following our procedures, we have:

$$f_{min} = 10.7 \text{ GHz},$$

$$f_{max} = 14.5 \text{ GHz}, \text{ or}$$

$$f_{max} \approx 1.36 f_{min}.$$

In this case, we choose

$$f_c = \sqrt{f_{min} f_{max}} = 12.46 \text{ GHz, and}$$

$$f_o = 1.02 f_c = 12.71 \text{ GHz.}$$

The input radius is chosen to be $a_i = \frac{3\lambda_c}{2\pi} = 11.49 \text{ mm}$. From Figure 3, we have $a_o \approx 1.95\lambda_c = 46.92 \text{ mm}$. The pitch is chosen to be $p = \frac{\lambda_c}{8} \approx 3 \text{ mm}$, with a pitch-to-width ratio $\delta = 0.8$ (i.e., the slots will be 2.4 mm wide, and the teeth will be 0.6 mm wide).

As $f_{max} \approx 1.36 f_{min}$, we choose a variable-depth-slot mode converter, with $\sigma = 0.42$. The length is chosen to be $L = 6\lambda_c = 60p \approx 180 \text{ mm}$, while we select a hyperbolic profile.

To work out the geometry of the horn, we need first to define the "stepped profile" of the horn, defined by N steps of length p , by following this procedure:

$$z_{step} = \frac{Np}{N-1} = \frac{L}{N-1}$$

do $j = 1, N$

$$z = (j-1)z_{step}$$

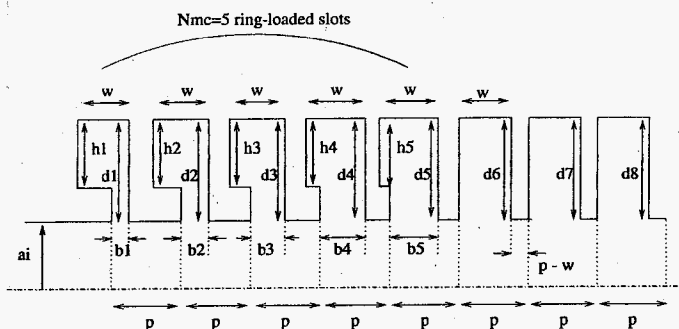


Figure 7. The detailed geometry of a mode converter with five ring-loaded slots.

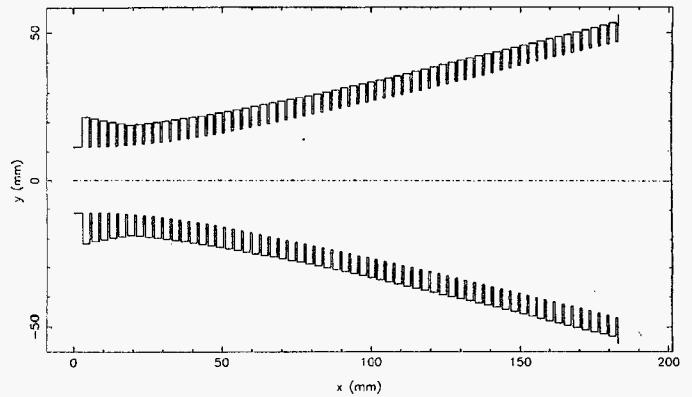


Figure 8. A corrugated horn with a variable-depth-slot mode converter.

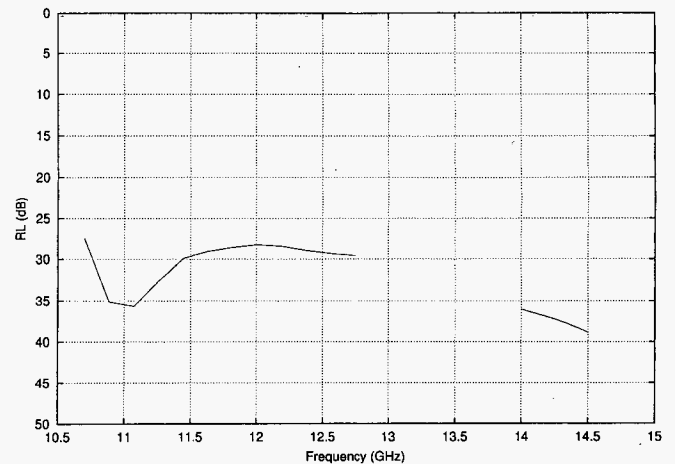


Figure 9. The return loss of the corrugated horn with a variable-depth-slot mode converter.

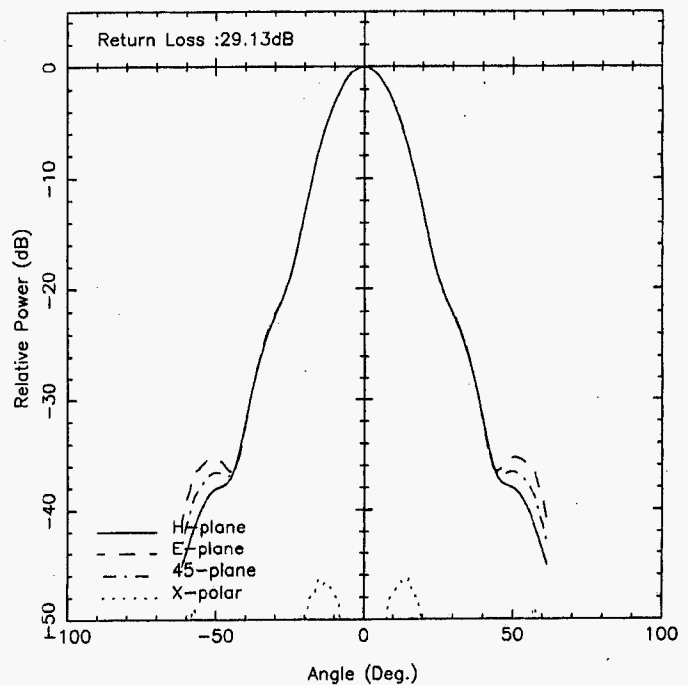


Figure 10a. The radiation pattern of a corrugated horn at Ku band: 12.46 GHz.

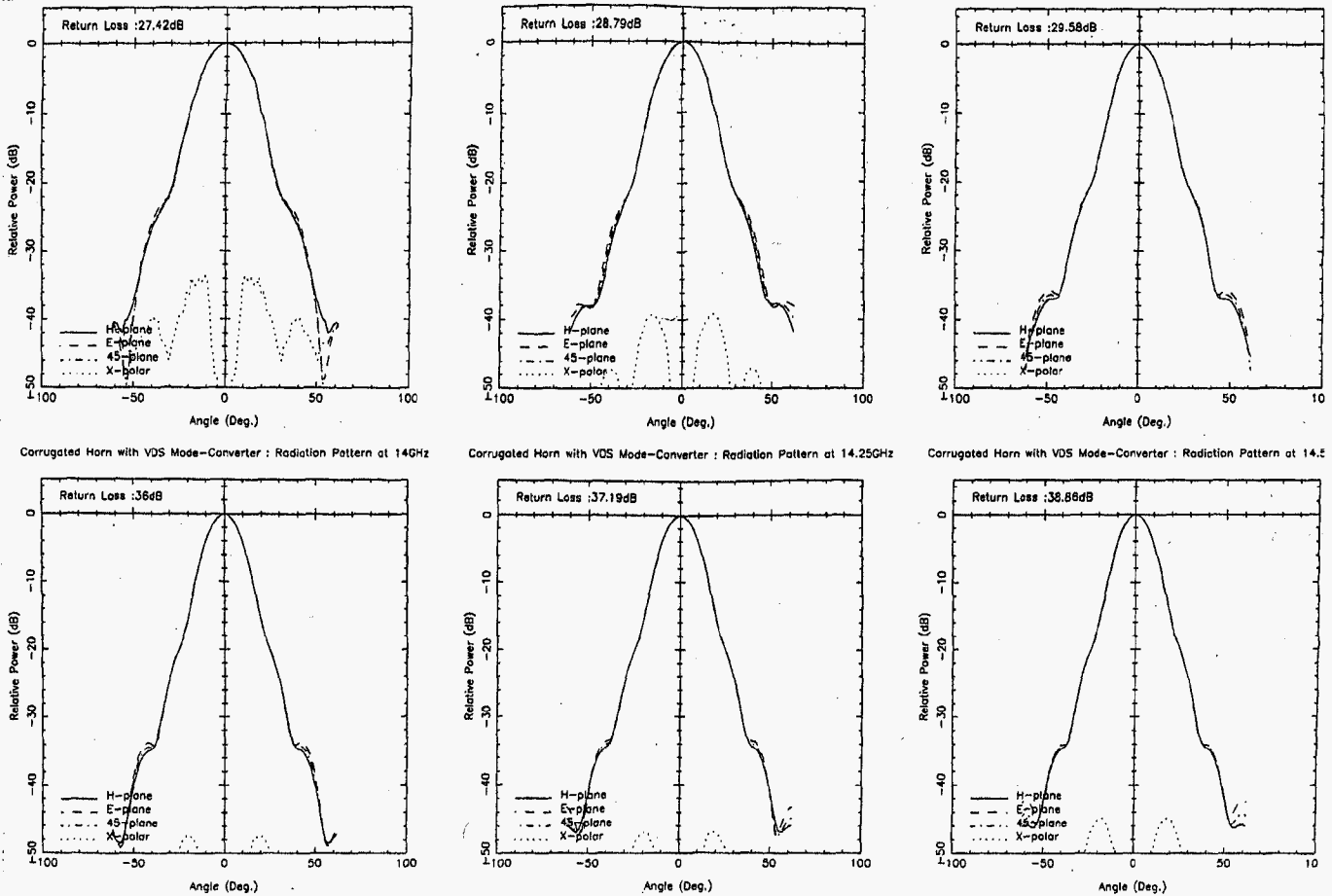


Figure 10b. The radiation pattern of a corrugated horn at Ku band: across the 10.7-12.75 GHz and 14.0-14.5 GHz bands.

$$a_j = \sqrt{a_i^2 + \frac{z^2(a_o^2 - a_i^2)}{L^2}}$$

(hyperbolic profile, any other profile can be used here)

end do

From this, we can devise a set of (radius = a_j , length = p) steps forming the basic stepped profile of the horn. Then, we need to use Table 2 to calculate the slot depth, d_j , associated with every a_j . The corrugated-horn geometry is then a set of N doublets of circular sections of finite lengths, defined like this:

$n = 0$

do $j = 1, N$

$radius_n = a_j + d_j$

$length_n = \delta p$

$radius_{n+1} = a_j$

(the profile is then formed of $2N$ cylindrical sections)

$length_{n+1} = (1 - \delta)p$

$n = n + 1$

end do

It is customary to add a section of length $\geq p$ and of radius a_i in front of the horn to simulate the input waveguide.

The geometry of the horn is shown in Figure 8. The return-loss performance is plotted in Figure 9, while the radiation pattern is shown in Figure 10. As can be seen from Figure 10a, the initial request of a horn radiation pattern with -15 dB at 20° at 12.46 GHz was basically met.

5. References

1. A. D. Olver, P. J. B. Clarricoats, A. A. Kishk, and L. Shafai, *Microwave Horns and Feeds*, London, IEE Electromagnetic Wave Series 39, 1994, ISBN 0 85296 809 4.
2. P. J. B. Clarricoats and A. D. Olver, *Corrugated Horns for Microwave Antennas*, London, IEE Electromagnetic Wave Series 18, 1984, ISBN 0 86341 003 0.
3. G. L. James, "Analysis and Design of TE11-to-HE11 Corrugated Cylindrical Waveguide Mode Converters," *IEEE Transactions on Antennas and Propagation*, Vol. AP-31, No. 1, January 1983.

tions on Microwave Theory and Techniques, MTT-29, 1981, pp. 1059-1066.

4. G. L. James and B. Mac Thomas, "TE₁₁₁-to-HE₁₁ Cylindrical Waveguide Mode Converters Using Ring-Loaded Slots," *IEEE Transactions on Microwave Theory and Techniques*, MTT-30, 3, March 1982, pp. 278-285.

5. G. L. James, "Design of Wide-Band Compact Corrugated Horns," *IEEE Transactions on Antennas and Propagation*, AP-32, 10, October 1984, pp. 1134-1138.

6. B. MacA Thomas, G. L. James, and K. J. Greene, "Design of Wide-Band Corrugated Conical Horns for Cassegrain Antennas," *IEEE Transactions on Antennas and Propagation*, AP-34, 6, June 1986, pp. 750-757.

7. B. MacA. Thomas B., "Design of Corrugated Conical Horns," *IEEE Transactions on Antennas and Propagation*, AP-26, 2, March 1978, pp. 367-372.

8. B. K. Watson, G. Y. Philipou, and N. Adatia, "Hybrid Mode Feeds for Multiband Applications," Colloquium on Multiband Techniques for Reflector Antennas, 1983, pp. 2/1-2/6.

9. X. Zhang, "Design of Conical Corrugated Feed Horns for Wide-Band High Frequency Applications," *IEEE Transactions on*

Microwave Theory and Techniques, MTT-41, 8, August 1993, pp. 1263-1274.

10. C. Granet, "Profile Options for Feed Horn Design," Proceedings of the Asia Pacific Microwave Conference, Vol. 1, 2000, pp. 1448-1452.

11. G. G. Gentili, E. Martini, R. Nesti, and G. Pelosi, "Performance Analysis of Dual Profile Corrugated Circular Waveguide Horns for Radioastronomy Applications," *IEE Proc.-Microw. Ant. & Prop.*, 148, 2, April 2001, pp. 119-122.

12. C. del Rio, R. Gonzalo, and M. Sorolla, "High Purity Gaussian Beam Excitation by Optimal Horn Design," Proceedings of ISAP'96, Chiba, Japan, pp. 1133-1136.

Ideas for Antenna Designer's Notebook

Ideas are needed for future issues of the Antenna Designer's Notebook. Please send your suggestions to Tom Milligan and they will be considered for publication as quickly as possible. Topics can include antenna design tips, equations, nomographs, or shortcuts, as well as ideas to improve or facilitate measurements. 

PATAR® Personal Antenna Range

A New Product Class Introduced by Farr Research

Our Portable Automated Time-domain Antenna Range, or **PATAR®** system, provides an economical turnkey solution for measuring both narrowband and wideband antennas from 900 MHz to 20 GHz. With no need for an anechoic chamber, the entire system can be quickly configured for indoor or outdoor use. A complete antenna measurement, including setup, alignment, measurement in two principal planes, signal processing, teardown, and stowage, can be completed within 4 hours.

The system includes our custom portable elevation/azimuth positioner, a fast sampling oscilloscope, a fast pulser, a laptop computer with software to drive the system and process the data, two calibration antennas, attenuators, and interconnecting cables.

The **PATAR®** system is easily used outdoors, since the instrumentation is relatively insensitive to temperature variations. Time gating is used to eliminate ground-bounce from the data. Our custom positioner is easily leveled and aligned, and it has a precision of better than ± 0.2 degrees.

We also offer a variety of ultra-wideband antennas, such as our Model IRA-3M, with bandwidth of 250 MHz to 20 GHz and impulse response with a full-width at-half-maximum of .32 ps.

**Farr
Research, Inc.**

For additional detail on all our products see our catalog, available at www.Farr-Research.com.
efarr@Farr-Research.com

